

Supporting Information for

Negative thermal expansion and linear compressibility in 1H-imidazol-3-i um 2-hydroxybenzoate with a helical network of hydrogen bonds

Sylwia Zięba,^{*1} Alina T. Dubis,² Michałina Rusek,³ Andrzej Katrusiak,³

Andrzej Gzella,⁴ Andrzej Łapiński¹

¹Institute of Molecular Physics, Polish Academy of Sciences, Smoluchowskiego 17, 60-179 Poznań, Poland

²Faculty of Chemistry, University of Białystok, Ciołkowskiego 1K, 15-245 Białystok, Poland

³Faculty of Chemistry, Adam Mickiewicz University, Uniwersytetu Poznańskiego 8, 61-614 Poznań, Poland

⁴Department of Organic Chemistry, Poznań University of Medical Sciences, Rokietnicka 3, 60-806 Poznań, Poland

*sylwia.zieba@ifmpan.poznan.pl

Figures

Figure S1. The second (red) and third-order (blue) Birch-Murnaghan equation of state for **SallMi**.

Figure S2. Two projections of chains of molecules linked by hydrogen bonds C3a–H3aa···O10bⁱⁱ into layers parallel to the *ab* plane.

Figure S3. A view of the unit cell of **SallMi** showing the double layers of molecules parallel to the *ab* plane. Adjacent double layers are shown in black and gray for clarity of drawing. The symmetry codes are explained in Table 1 and Fig. 3. *Cg1* is a phenylene ring centroid; Ph and Im are phenylenes and imidazolium rings. Symmetry codes: (iii) 3/2-*x*, 1-*y*, 1/2+*z*, (iv) 1-*x*, 1-*y*, 1-*z*.

Figure S4. (a) The C–H···*Cg* and (b) π ··· π interactions; the shaded area highlights the degree of overlap of the Ph and Im rings; *Cg1* is phenylene ring centroid; Ph and Im are phenylene and imidazolium rings. H atoms not involved in hydrogen bonding have been omitted for clarity. Symmetry code: (iv) 1-*x*, 1-*y*, 1-*z*.

Figure S5. Raman spectra of imidazolium salicylate under temperature in three spectral regions: 20–220 (left), 760–920 (middle), and 1420–1660 cm⁻¹ (right).

Figure S6. Raman spectra of imidazolium salicylate under pressure in two spectral regions: 950–650 (left) and 180–50 cm⁻¹ (right).

Figure S7. Calculated FT-IR (a) and Raman (b) spectra of imidazolium and acid ions; scaling factor of 0.97, DFT method: ωB97XD/6-311++G(d,p).

Figure S8. Temperature evolution of the lengths of C···O in the C–H···O hydrogen bond (a) and O···O in the O–H···O hydrogen bond (b). The evolution of the position of the bands at 757 and 768 cm⁻¹ (a) and 1346 cm⁻¹ (b) is shown on the right.

Figure S9. Pressure evolution of C···O lengths in C–H···O hydrogen bond (a) and O···O in O–H···O hydrogen bond (b).

Figure S10. Crystal structure of imidazolium salicylate. The dotted lines denote the axes where the imidazolium ion rotates in the crystal.

Figure S11. Values of anharmonic factor $\psi(A)$ (a), damping parameter $\Delta v/v_0$, and the maximum absorption energy $F[A_c(v_0)]$ (b) of imidazolium salicylate as a function of temperature.

Tables

Table S1. Crystal data, data collection, and structure refinement for **SalImi** at different temperatures at atmospheric pressure.

Table S2. Crystal data, data collection, and structure refinement for **SalImi** at different pressures at room temperature ($T=293.02$ K).

Table S3. Cell parameters (\AA , $^\circ$) for **SalImi** at different temperatures (K).

Table S4. Cell parameters (\AA , $^\circ$) for **SalImi** at different pressures (GPa).

Table S5. The second and third-order Birch-Murnaghan coefficient of volume under pressure for **SalImi**: B_0 (GPa) - the bulk modulus, B'_0 the bulk modulus pressure derivative, V_0 (\AA^3) the unit cell volume at ambient conditions, and with σ their standard errors.

Table S6. Hydrogen-bonds and C—H \cdots Cg interactions (\AA , $^\circ$) in the crystal structure of **SalImi** at different temperatures.

Table S7. Hydrogen bond geometry (\AA , $^\circ$) for **SalImi** at different pressures.

Table S8. **SalImi** QTAIM parameters (in atomic unit) as a function of temperature corresponding to the H \cdots O bond critical point (BCPs), the electron density at BCP ρ_{BCP} ; Laplacian of electron density at BCP, $\Delta\rho_{\text{BCP}}$; total electron energy density at BCP, H_{BCP} and the components of the H_{BCP} : kinetic electron energy density, G_{BCP} ; potential electron energy density, V_{BCP} , the hydrogen bond energy, E_{HB} ($\text{kcal}\cdot\text{mol}^{-1}$).

Table S9. **SalImi** QTAIM parameters (in atomic unit) as a function of pressure corresponding to the H \cdots O bond critical point (BCPs), the electron density at BCP ρ_{BCP} ; Laplacian of electron density at BCP, $\Delta^2\rho_{\text{BCP}}$; total electron energy density at BCP, H_{BCP} and the components of the H_{BCP} : kinetic electron energy density, G_{BCP} ; potential electron energy density, V_{BCP} , the hydrogen bond energy, E_{HB} .

Table S10. Parameters of the helicoid: a_h (semi-major axis), b_h (semi-minor axis), Sh_h (helix pitch), c_h (focal length of the ellipse), e_h (eccentricity of the ellipse), l_h (circumference of the ellipse), and S_h (area of the ellipse).

Table S11. The assignment of the selected vibrational bands observed in FT-IR and Raman spectra of **SalImi**.

Table S12. The assignment of the selected bands observed in Raman spectra in the phonon spectral range of **SalImi**.

Table S13. Lengths and angles of the bonds in the imidazole ion as a function of the temperature. Note: The atomic labeling scheme is shown in Figure 1.

Table S14. Lengths and angles of the bonds in the imidazole ion as a function of the pressure. Note: The atomic labeling scheme is shown in Figure 1.

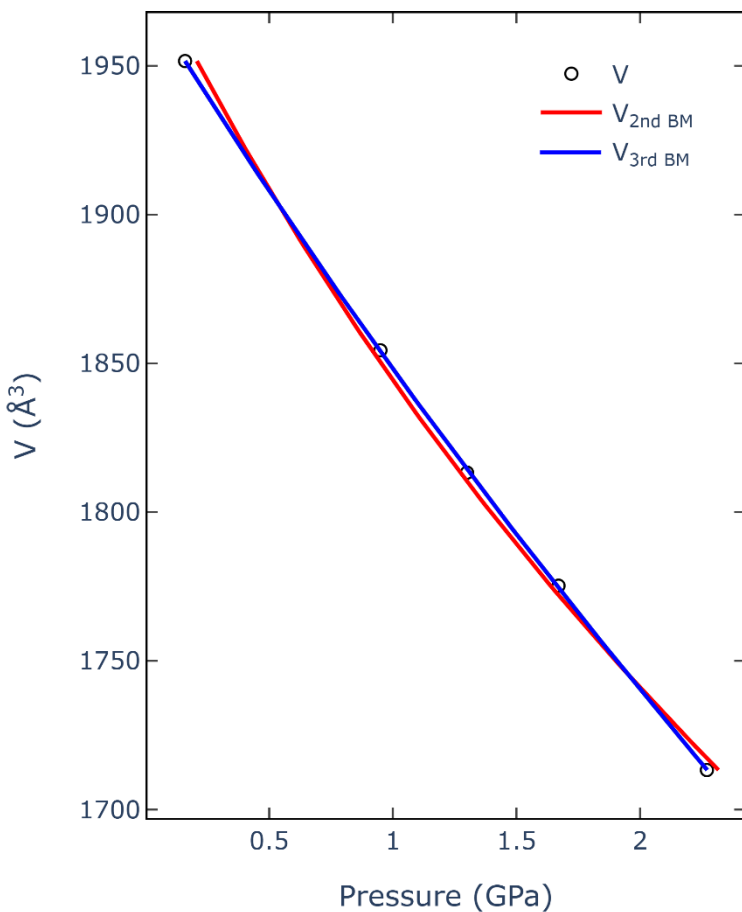


Figure S1. The second (red) and third-order (blue) Birch-Murnaghan equation of state for **SalImi**. \circ V – Experimental Cell Volume; The red and blue solid lines are, respectively, fits of the second (described as $V_{2\text{nd BM}}$) and third-order B-M equation ($V_{3\text{rd BM}}$) to the experimental points.

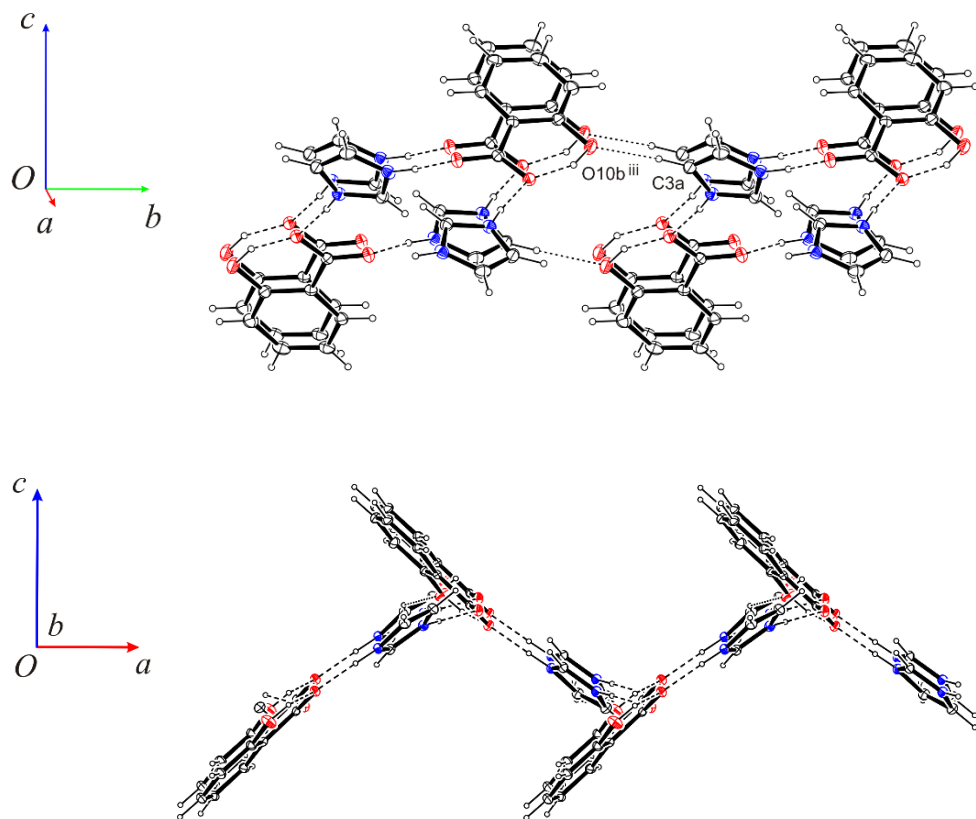


Figure S2. Two projections of chains of molecules linked by hydrogen bonds $\text{C}3\text{a}-\text{H}3\text{aa}\cdots\text{O}10\text{b}^{\text{ii}}$ into layers parallel to the ab plane.

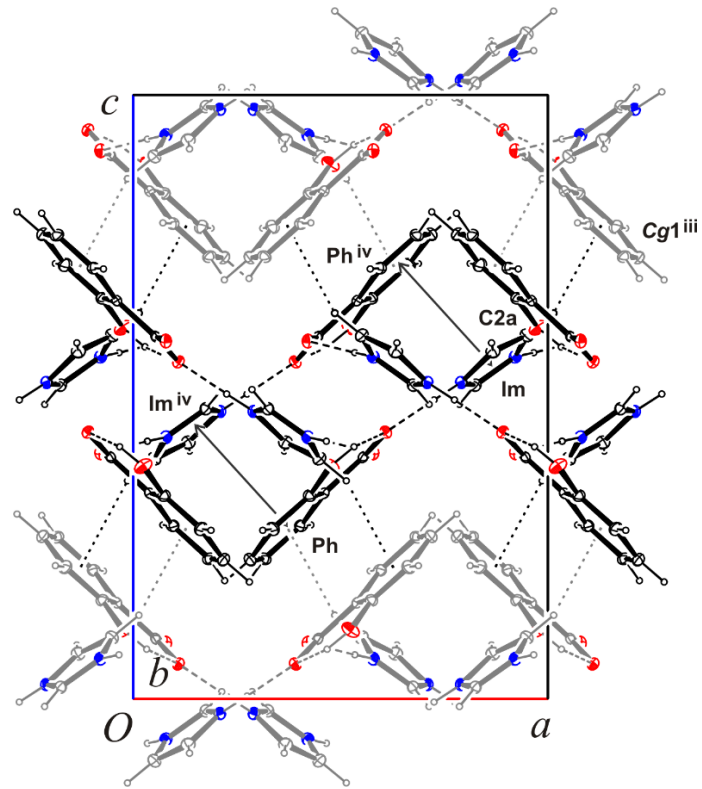
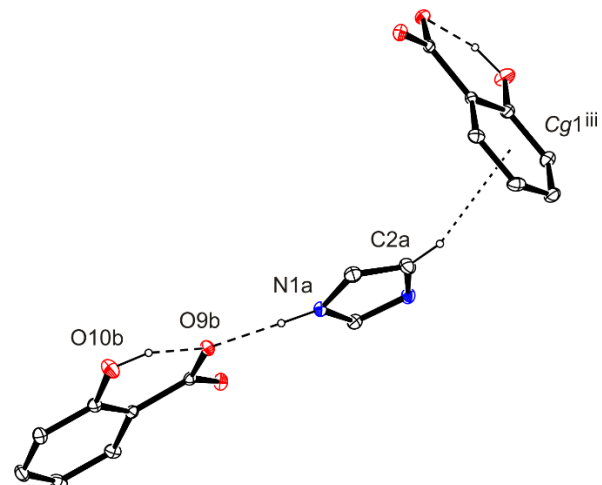


Figure S3. A view of the unit cell of **SalImi** showing the double layers of molecules parallel to the ab plane. Adjacent double layers are shown in black and gray for clarity of drawing. The symmetry codes are explained in Table 1 and Fig. 3a. $Cg1$ is a phenylene ring centroid; Ph and Im are phenylenes and imidazolium rings. Symmetry codes: (iii) $3/2-x, 1-y, 1/2+z$, (iv) $1-x, 1-y, 1-z$.

a)



b)

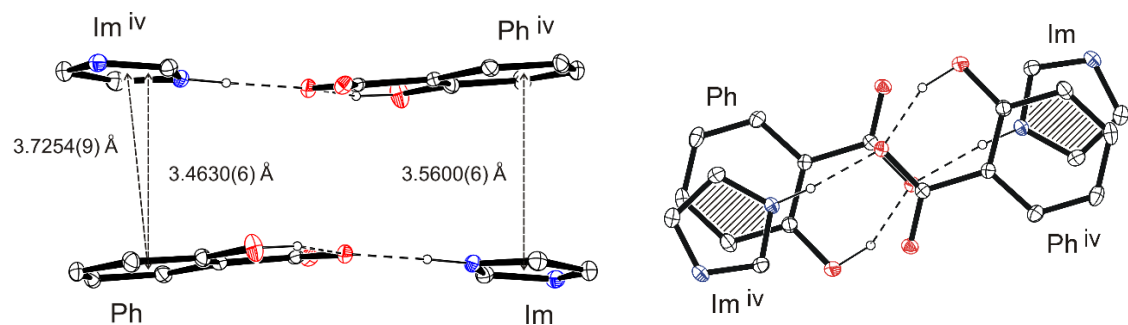


Figure S4. (a) The C–H \cdots Cg and (b) $\pi\cdots\pi$ interactions; the shaded area highlights the degree of overlap of the Ph and Im rings; Cg1 is phenylene ring centroid; Ph and Im are phenylene and imidazolium rings. H atoms not involved in hydrogen bonding have been omitted for clarity. Symmetry code: (iv) 1-x, 1-y, 1-z.

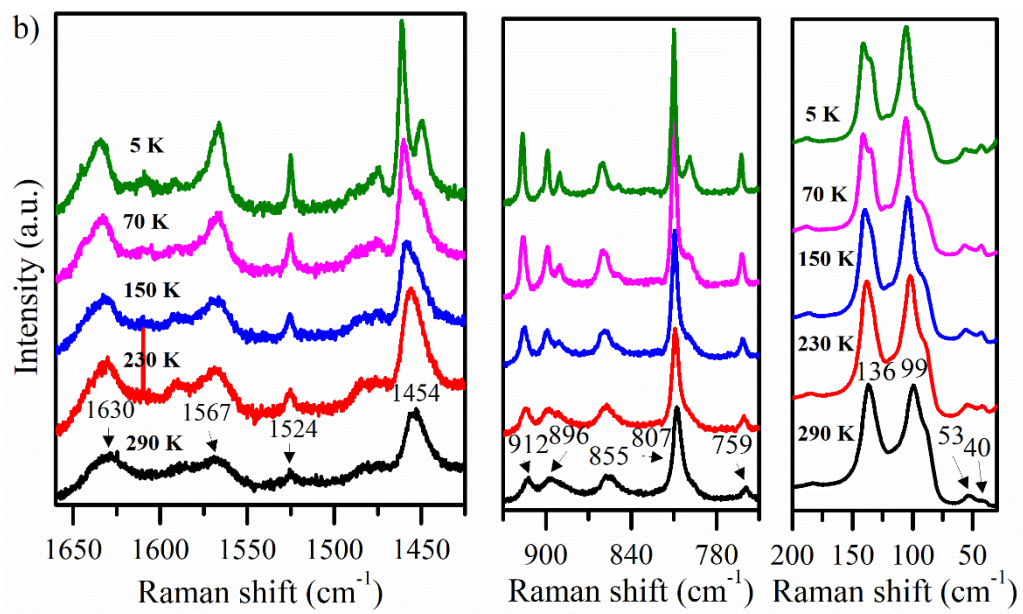


Figure S5. Raman spectra of imidazolium salicylate under temperature in three spectral regions: 20–220 (left), 760–920 (middle), and 1420–1660 cm^{-1} (right).

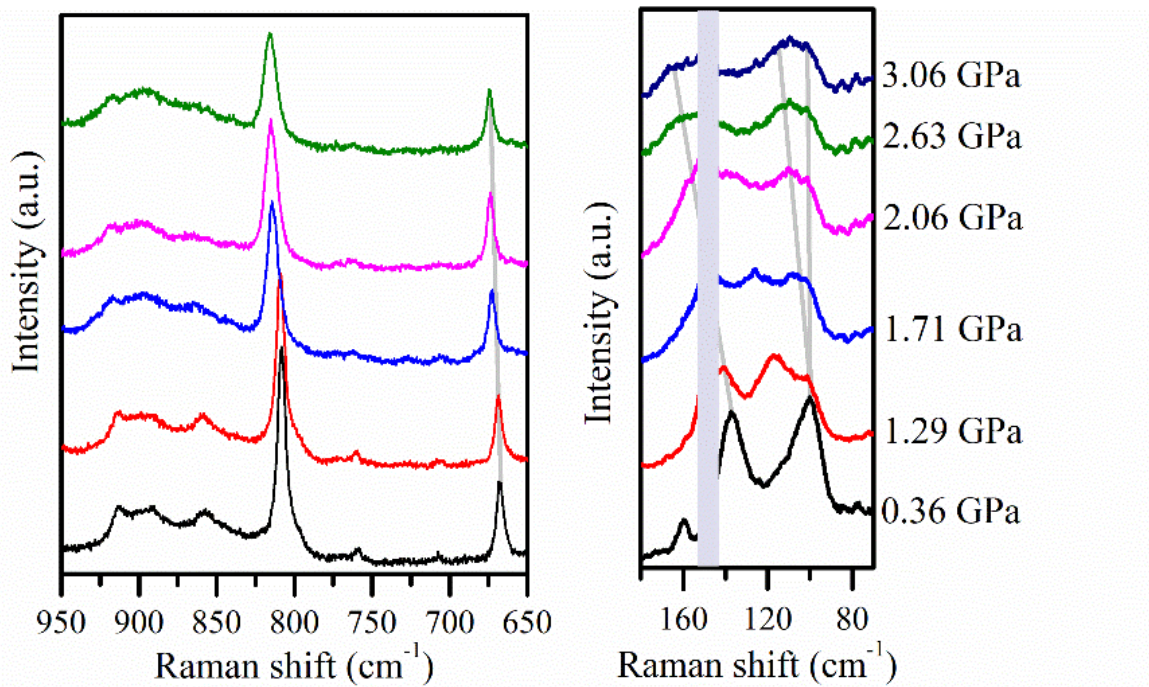


Figure S6. Raman spectra of imidazolium salicylate under pressure in two spectral regions: 950–650 (left) and 180–50 cm^{-1} (right).

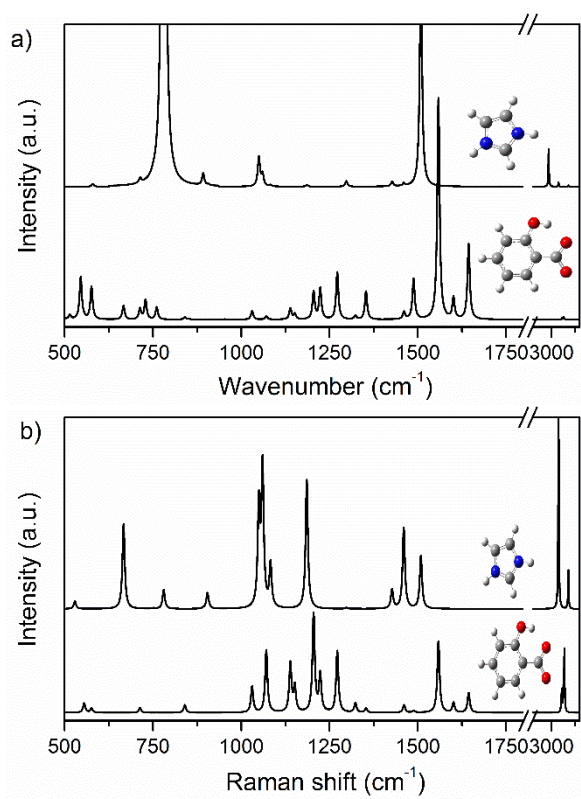


Figure S7. Calculated FT-IR (a) and Raman (b) spectra of imidazolium and acid ions; scaling factor of 0.97, DFT method: $\omega\text{B97XD}/6-311++\text{G}(\text{d},\text{p})$.

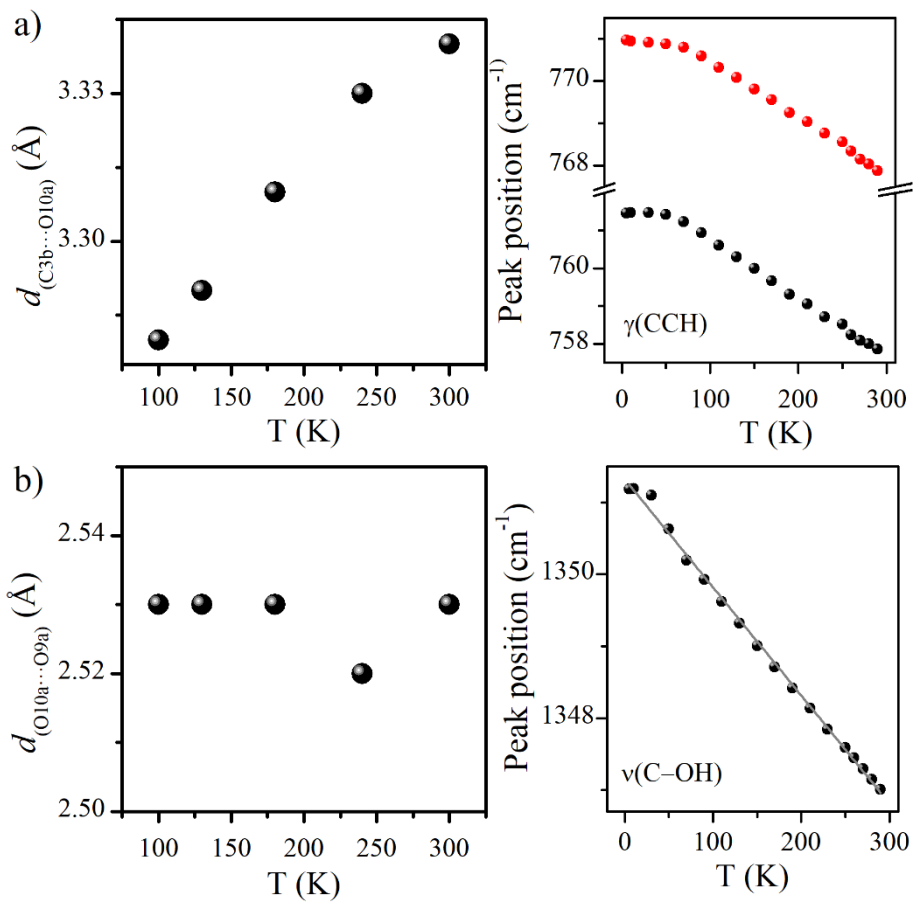


Figure S8. Temperature evolution of the lengths of C···O in the C–H···O hydrogen bond (a) and O···O in the O–H···O hydrogen bond (b). The evolution of the position of the bands at 757 and 768cm⁻¹ (a) and 1346cm⁻¹ (b) is shown on the right.

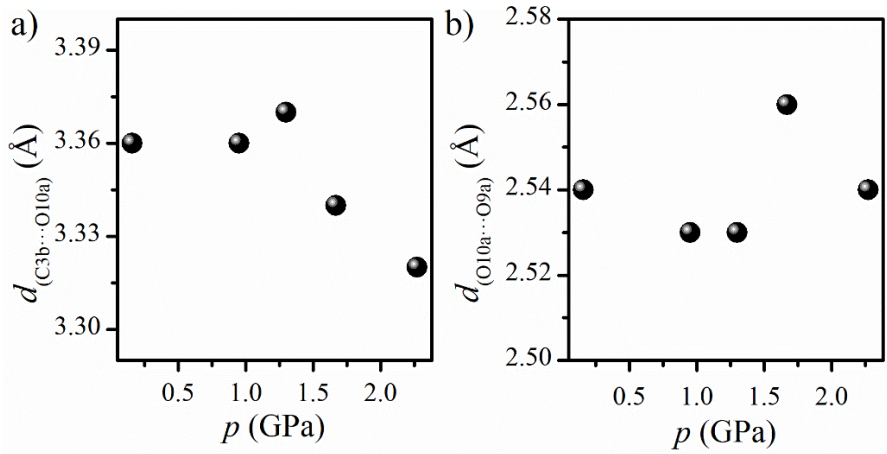


Figure S9. Pressure evolution of C \cdots O lengths in C–H \cdots O hydrogen bond (a) and O \cdots O in O–H \cdots O hydrogen bond (b).

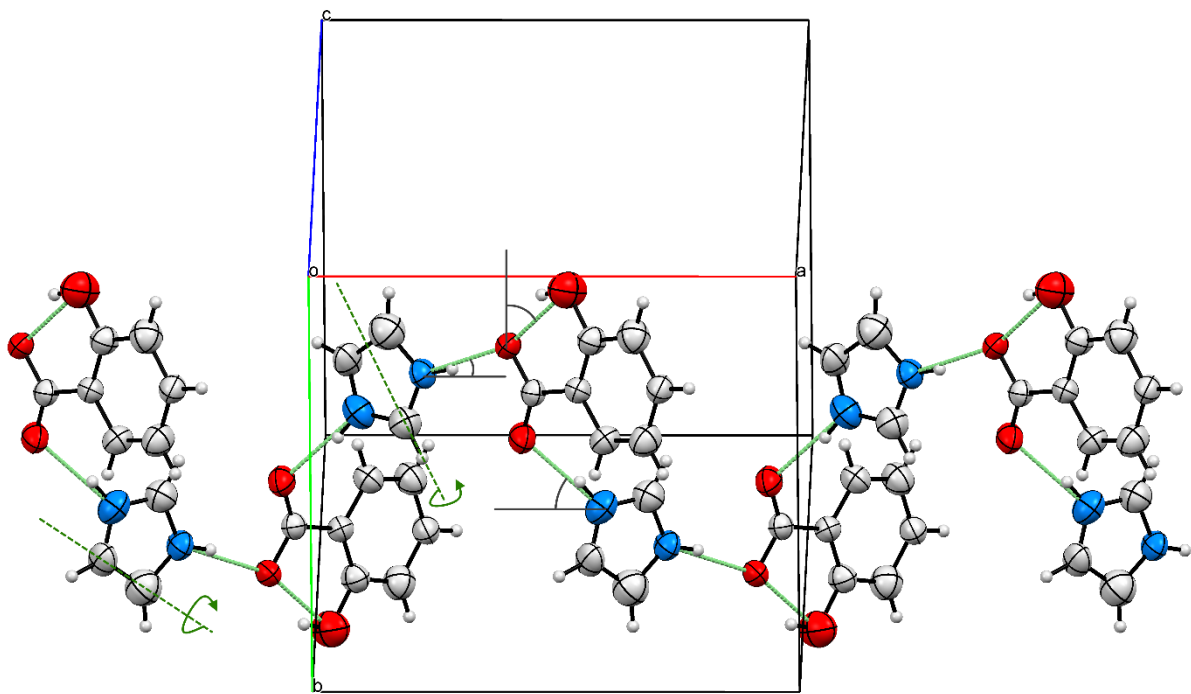


Figure S10. Crystal structure of imidazolium salicylate. The dotted lines denote the axes where the imidazolium ion rotates in the crystal.

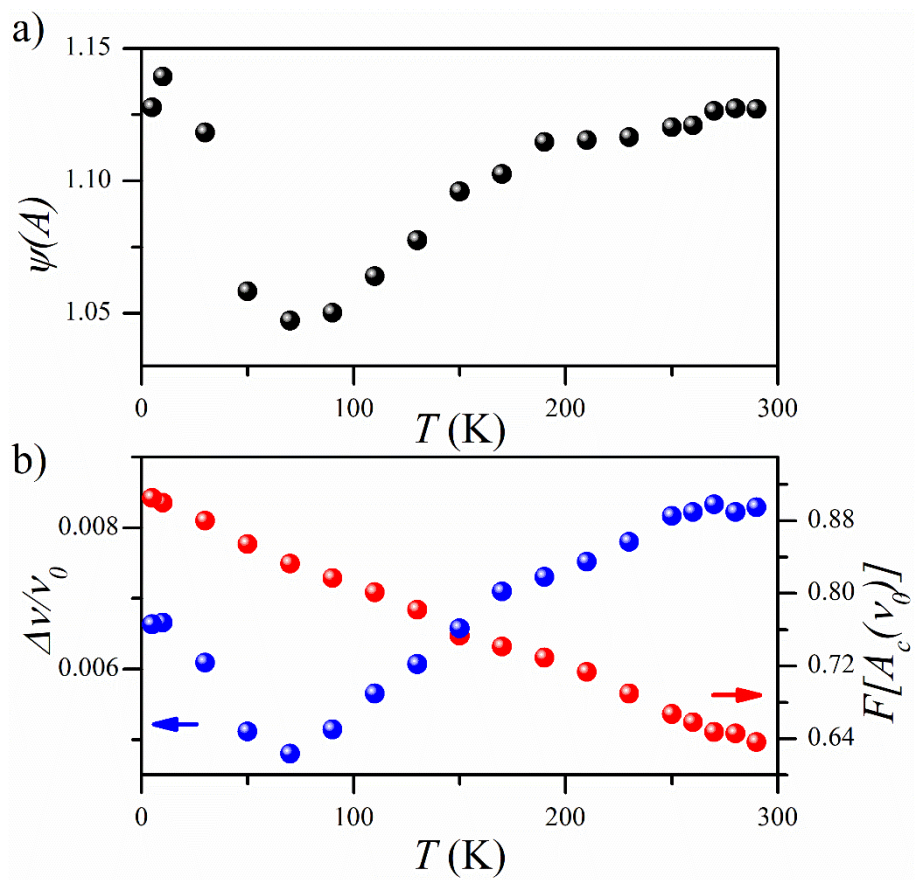


Figure S11. Values of anharmonic factor $\psi(A)$ (a), damping parameter $\Delta\nu/\nu_0$, and the maximum absorption energy $F[A_c(\nu_0)]/I$ (b) of imidazolium salicylate as a function of temperature.

Table S1. Crystal data, data collection, and structure refinement for **Sallmi** at different temperatures at atmospheric pressure

Crystal data					
Chemical formula	C ₁₀ H ₁₀ N ₂ O ₃	C ₁₀ H ₁₀ N ₂ O ₃	C ₁₀ H ₁₀ N ₂ O ₃	C ₁₀ H ₁₀ N ₂ O ₃	C ₁₀ H ₁₀ N ₂ O ₃
M _r	206.20	206.20	206.20	206.20	206.20
Crystal system, space group	Orthorhombic, <i>Pbca</i>				
Temperatur (K)	100.0(1)	130.0(1)	180.0(1)	240.0(1)	300.0(1)
Unit cell parameters					
<a> (Å)	11.0676(5)	11.0905(6)	11.1043(5)	11.0988(6)	11.0777(11)
b (Å)	11.0227(5)	10.9922(5)	10.9664(5)	10.9361(5)	10.9375(9)
c (Å)	16.1520(7)	16.1833(8)	16.3069(9)	16.4701(9)	16.6880(15)
α, β, γ (°)	90, 90, 90	90, 90, 90	90, 90, 90	90, 90, 90	90, 90, 90
V (Å ³)	1970.45(15)	1972.89(16)	1985.76(17)	1999.10(18)	2022.0(3)
Z	8	8	8	8	8
F(000)	864	864	864	864	864
D _x (Mg m ⁻³)	1.390	1.388	1.379	1.370	1.355
Radiation type, λ(Å)			Mo <i>K</i> α, 0.71073		
μ (mm ⁻¹)	0.105	0.105	0.104	0.103	0.102
Crystal shape			Block		
Color			Colourless		
Crystal size (mm)			0.30 x 0.26 x 0.13		
Data collection					
Diffractometer	SuperNova, Dual Mo, Atlas	SuperNova, Dual Mo, Atlas	SuperNova, Dual Mo, Atlas	SuperNova, Dual Mo, Atlas	SuperNova, Dual Mo, Atlas
Absorption correction	Multi-scan (CrysAlis PRO). Empirical absorption correction using spherical harmonics, implemented in SCALE3 ABSPACK scaling algorithm.				
T _{min} , T _{max}	0.700, 1.000	0.628, 1.000	0.640, 1.000	0.626, 1.000	0.582, 1.000
No. of measured, independent and observed [I > 2σ(I)] reflections	16383, 2561, 2214	16447, 2578, 2173	16741, 2567, 2058	16879, 2584, 1913	15447, 2617, 1775
Measurement method	ω scans				
R _{int}	0.0274	0.0360	0.0340	0.0334	0.0375
θ _{max} , θ _{min} (°)	29.51, 2.90	29.60, 2.52	29.64, 2.89	29.67, 2.89	29.66, 2.44
Structure refinement					
R [F ² ≥ 2σ(F ²)], wR(F ²), S	0.0400, 0.1033, 1.080	0.0450, 0.1222, 1.087,	0.0465, 0.1153, 1.077	0.0493, 0.1362, 1.074	0.0524, 0.1418, 1.067
No. of reflections	2561	2578	2567	2584	2617
No. of parameters	148	148	149	149	149
Δρ _{max} , Δρ _{min} (e Å ⁻³)	0.291, -0.267	0.261, -0.313	0.364, -0.182	0.323, -0.181	0.249, -0.219
Extinction correction	$F_c^* = kF_c[1 + 0.001xF_c^2\lambda^3/\sin(2\theta)]^{-1/4}$				
Extinction coefficient	–	–	0.0069(9)	0.0075(11)	0.0121(14)

Table S2. Crystal data, data collection, and structure refinement for **Sallmi** at different pressures at room temperature ($T=293.02$ K).

Chemical formula	C ₁₀ H ₉ N ₂ O ₃	C ₁₀ H ₉ N ₂ O ₃	C ₁₀ H ₉ N ₂ O ₃	C ₁₀ H ₉ N ₂ O ₃	C ₁₀ H ₉ N ₂ O ₃
Formula weight	206.19	206.19	206.19	206.19	206.19
Pressure (GPa)	0.16	0.95	1.30	1.67	2.27
Wavelength (Å)	0.71073	0.71073	0.71073	0.71073	0.71073
Crystal system	Orthorhombic	Orthorhombic	Orthorhombic	Orthorhombic	Orthorhombic
Space group	<i>Pbca</i>	<i>Pbca</i>	<i>Pbca</i>	<i>Pbca</i>	<i>Pbca</i>
Unit cell parameters (Å, °)	a=11.2640(13) b=10.812(11) c=16.025(2)	a=11.4739(8) b=10.652(7) c=15.1725(13)	a=11.5502(8) b=10.596(7) c=14.8160(13)	a=11.562(3) b=10.656(19) c=14.409(3)	a=11.540(5) b=10.49(4) c=14.153(8)
Volume (Å ³)	1952(2)	1854.4(12)	1813.3(12)	1775(3)	1713(7)
Z	8	8	8	8	8
<i>F</i> (000)	864.0	864.0	864.0	864.0	864.0
Calculated density (g cm ⁻³)	1.404	1.477	1.511	1.543	1.599
Absorption coefficient (mm ⁻¹)	0.106	0.111	0.114	0.116	0.120
Crystal dimensions [mm]			0.20 x 0.18 x 0.13		
Θ Range for data collection (°)	4.625 to 26.634	4.773 to 24.757	4.841 to 21.998	4.495 to 19.579	4.956 to 27.269
Max./Min. indices	h:-13→13 k:-4→4 l:-19→19	h:-14→14 k:-4→4 l:-18→18	h:-14→14 k:-4→4 l:-18→18	h:-14→14 k:-4→4 l:-17→17	h:-14→14 k:-3→3 l:-17→17
Ref. collected/unique	7165/792	7603/744	7442/732	6634/612	5289/576
Observed reflections [$I \geq 2\sigma(I)$]	1007	1207	1257	702	581
R _{int}	0.1218	0.0830	0.0787	0.1062	0.1165
Parameters	138	137	137	137	118
final R indices [$I > 2\sigma(I)$]	$R_1=0.0743$ $wR_2=0.1879$	$R_1=0.0535$ $wR_2=0.1264$	$R_1=0.0553$ $wR_2=0.1273$	$R_1=0.0743$ $wR_2=0.1963$	$R_1=0.0987$ $wR_2=0.2377$
R indices (all data)	$R_1=0.1702$ $wR_2=0.2554$	$R_1=0.1336$ $wR_2=0.1688$	$R_1=0.1407$ $wR_2=0.1712$	$R_1=0.2221$ $wR_2=0.2991$	$R_1=0.2370$ $wR_2=0.3536$
goodness of fit of F^2	1.012	1.014	1.018	1.018	1.048
Largest diff. peak and hole	0.13/-0.14	0.12/-0.17	0.13/-0.16	0.14/-0.16	0.21/-0.18

Table S3. Cell parameters (\AA , $^\circ$) for **SalImi** at different temperatures (K).

Temperature	<i>a</i>	<i>b</i>	<i>c</i>	α	β	γ	<i>V</i>
100	11.0676(5)	11.0227(5)	16.1520(7)	90.00	90.00	90.00	1970.46(15)
130	11.0905(6)	10.9922(5)	16.1833(8)	90.00	90.00	90.00	1972.89(16)
180	11.1043(5)	10.9664(5)	16.3069(9)	90.00	90.00	90.00	1985.76(17)
240	11.0988(6)	10.9361(5)	16.4701(9)	90.00	90.00	90.00	1999.10(18)
300	11.0777(11)	10.9375(9)	16.6880(15)	90.00	90.00	90.00	2022.0(3)

Table S4. Cell parameters (\AA , $^\circ$) for **SalImi** at different pressures (GPa).

Pressure	<i>a</i>	<i>b</i>	<i>c</i>	α	β	γ	<i>V</i>
0.16	11.2640(13)	10.812(11)	16.025(2)	90.00	90.00	90.00	1952(2)
0.95	11.4739(8)	10.652(7)	15.1725(13)	90.00	90.00	90.00	1854.4(12)
1.30	11.5502(8)	10.596(7)	14.8160(13)	90.00	90.00	90.00	1813.3(12)
1.67	11.562(3)	10.656(19)	14.409(3)	90.00	90.00	90.00	1775(3)
2.27	11.540(5)	10.49(4)	14.153(8)	90.00	90.00	90.00	1713(7)

Table S5. The second and third-order Birch-Murnaghan coefficient of volume under pressure for SalImi: B_0 (GPa) - the bulk modulus, B_0' the bulk modulus pressure derivative, V_0 (\AA^3) the unit cell volume at ambient conditions, and with σ their standard errors.

	B_0 (GPa)	σB_0 (GPa)	V_0 (\AA^3)	σV_0 (\AA^3)	B_0'	$\sigma B_0'$
2nd	11.7	0.5	1985.4	7.7	4.0	0
3rd	14.5	0.3	1973.1	1.5	1.8	0.2

Table S6. Hydrogen-bonds and C–H···Cg interactions (Å, °) in the crystal structure of **Sallmi** at different temperatures.

Temperature (K)	D—H···A	D—H (Å)	H···A (Å)	D···A (Å)	D—H···A (°)
100		0.93(2)	1.77(2)	2.6903(13)	174.6(18)
		0.95(2)	1.74(2)	2.6779(13)	165.7(19)
		0.98(2)	1.61(2)	2.5300(13)	155(2)
		0.95	2.41	3.2545(16)	148
130		0.93(2)	1.77(2)	2.6950(15)	173(2)
		0.93(2)	1.77(2)	2.6798(15)	166(2)
		0.96(2)	1.62(2)	2.5285(14)	156(2)
		0.95	2.42	3.2537(18)	147
180	N1a—H1a···O9b N2a—H2a···O8b ⁱ O10b—H10b···O9b C3a—H3aa···O10b ⁱⁱ	0.92(2)	1.80(2)	2.7079(16)	172(2)
		0.93(2)	1.78(2)	2.6873(17)	167(2)
		0.98(2)	1.60(2)	2.5275(16)	156(2)
		0.95	2.44	3.266(2)	145
240		0.92(3)	1.81(3)	2.7199(19)	171(2)
		0.93(2)	1.77(2)	2.692(2)	170(2)
		1.01(2)	1.56(2)	2.5245(19)	157(2)
		0.94	2.47	3.278(2)	144
300		0.94(3)	1.80(3)	2.731(2)	169(2)
		0.92(3)	1.79(3)	2.701(2)	170(3)
		1.05(3)	1.54(3)	2.525(2)	156(3)
		0.93	2.51	3.303(3)	143
Temperature (K)	C—H···Cg	C—H (Å)	H···Cg (Å)	C···Cg (Å)	C—H···Cg (°)
100	C2a—H2aa···Cg1 ⁱⁱⁱ	0.95	2.68	3.5667(14)	156
130		0.95	2.69	3.5777(16)	156
180		0.95	2.72	3.6067(18)	156
240		0.94	2.77	3.645(2)	156
300		0.93	2.82	3.689(2)	156

Symmetry codes: (i) $-1/2+x, 3/2-y, 1-z$; (ii) $-1/2+x, 1/2-y, 1-z$; (iii) $3/2-x, 1-y, 1/2+z$. Cg1 is phenyl ring centroid.

Table S7. Hydrogen bond geometry (\AA , $^\circ$) for **SalImi** at different pressures.

Pressure (GPa)	$D\text{--H}\cdots A$	$D\text{--H}$	$H\cdots A$	$D\cdots A$	$D\text{--H}\cdots A$
0.16		0.86(1)	1.89(1)	2.737(13)	169.9(12)
		0.86(1)	1.84(1)	2.700(20)	174.2(8)
		0.82(1)	1.85(1)	2.544(15)	141.3(10)
		0.93(2)	2.35(1)	3.120(30)	140.2(7)
0.95		0.86(1)	1.86(1)	2.698(9)	168.0(8)
		0.86(1)	1.86(1)	2.711(15)	168.7(7)
		0.82(1)	1.81(1)	2.527(11)	144.7(8)
		0.93(2)	2.38(1)	3.138(19)	138.9(5)
1.30	N1a–H1a…O9b N2a–H2a…O8b ⁱ O10b–H10b…O9b C3a–H3aa…O10b ⁱⁱ	0.86(1)	1.86(1)	2.697(10)	163.2(9)
		0.86(1)	1.84(1)	2.680(17)	166.6(7)
		0.82(1)	1.85(1)	2.548(9)	142.4(8)
		0.93(2)	2.33(1)	3.061(21)	135.3(6)
1.67		0.86(1)	1.86(1)	2.685(18)	161.2(15)
		0.86(2)	1.85(1)	2.682(31)	163.5(11)
		0.82(1)	1.90(1)	2.561(20)	136.5(13)
		0.93(3)	2.28(1)	3.011(42)	135.2(12)
2.27		0.86(1)	1.88(1)	2.701(18)	159.4(16)
		0.86(3)	1.83(1)	2.663(33)	164.5(12)
		0.82(1)	1.81(1)	2.513(21)	143.5(13)
		0.93(4)	2.28(1)	2.990(40)	132.9(12)

Symmetry codes: (i) $-1/2+x, 3/2-y, 1-z$; (ii) $-1/2+x, 1/2-y, 1-z$; (iii) $1/2-x, 1-y, 1/2+z$.

Table S8. SalImi QTAiM parameters (in atomic unit) as a function of temperature corresponding to the H \cdots O bond critical point (BCPs), the electron density at BCP ρ_{BCP} ; Laplacian of electron density at BCP, $\Delta\rho_{\text{BCP}}$; total electron energy density at BCP, H_{BCP} and the components of the H_{BCP} : kinetic electron energy density, G_{BCP} ; potential electron energy density, V_{BCP} , the hydrogen bond energy, E_{HB} (kcal \cdot mol $^{-1}$).

	T (K)	ρ_{BCP}	$\Delta\rho_{\text{BCP}}$	G_{BCP}	V_{BCP}	H_{BCP}	E_{HB}
O10b-H10b \cdots O9b	100	0.0590	0.1655	0.0521	-0.0628	-0.0107	-19.69
	130	0.0574	0.1668	0.0513	-0.0609	-0.0096	-19.12
	180	0.0613	0.1659	0.0535	-0.0656	-0.0121	-20.58
	240	0.0631	0.1648	0.0544	-0.0676	-0.0132	-21.22
	300	0.0663	0.1619	0.0559	-0.0713	-0.0154	-22.37
N1a-H1a \cdots O9b	100	0.0394	0.1333	0.0345	-0.0358	-0.0012	-11.22
	130	0.0396	0.1317	0.0344	-0.0358	-0.0014	-11.23
	180	0.0370	0.1279	0.0324	-0.0328	-0.0004	-10.29
	240	0.0352	0.1241	0.0308	-0.0306	0.0002	-9.58
	300	0.0363	0.1218	0.0309	-0.0314	-0.0005	-9.85
N2a-H2a \cdots O8b ⁱ	100	0.0396	0.1436	0.0365	-0.0370	-0.0006	-11.62
	130	0.0378	0.1423	0.0353	-0.0350	0.0003	-10.99
	180	0.0367	0.1400	0.0344	-0.0337	0.0007	-10.57
	240	0.0372	0.1403	0.0347	-0.0343	-0.0004	-10.75
	300	0.0344	0.1362	0.0325	-0.0310	0.0015	-9.74

Table S9. SalImi QTAIM parameters (in atomic unit) as a function of pressure corresponding to the H \cdots O bond critical point (BCPs), the electron density at BCP ρ_{BCP} ; Laplacian of electron density at BCP, $\Delta^2\rho_{\text{BCP}}$; total electron energy density at BCP, H_{BCP} and the components of the H_{BCP} : kinetic electron energy density, G_{BCP} ; potential electron energy density, V_{BCP} , the hydrogen bond energy, E_{HB} .

p (GPa)	ρ_{BCP}	Δ_{BCP}	G_{BCP}	V_{BCP}	H_{BCP}	E_{HB}	
O10b-H10b \cdots O9b	0.16	0.0354	0.1457	0.0353	-0.0341	0.0012	-10.71
	0.95	0.0357	0.1456	0.0354	-0.0344	0.0009	-10.79
	1.30	0.0347	0.1430	0.0345	-0.0332	0.0013	-10.41
	1.67	0.0315	0.1308	0.0308	-0.0289	0.0019	-9.07
	2.27	0.0315	0.1353	0.0316	-0.0294	0.0022	-9.22
N1a-H1a \cdots O9b	0.16	0.0305	0.1152	0.0271	-0.0254	0.0017	-7.96
	0.95	0.0327	0.1251	0.0297	-0.0282	0.0015	-8.85
	1.30	0.0326	0.1243	0.0295	-0.0279	0.0015	-8.78
	1.67	0.0325	0.1288	0.0303	-0.0284	0.0019	-8.91
	2.27	0.0370	0.1401	0.0344	-0.0337	0.0006	-10.58
N2a-H2a \cdots O8b ⁱ	0.16	0.0315	0.1354	0.0309	-0.0281	0.0029	-8.82
	0.95	0.0307	0.1291	0.0295	-0.0267	0.0028	-8.36
	1.30	0.0322	0.1359	0.0313	-0.0287	0.0027	-9.00
	1.67	0.0322	0.1317	0.0306	-0.0283	0.0023	-8.87
	2.27	0.0359	0.1516	0.0359	-0.0339	0.0020	-10.64

Table S10. Parameters of the helicoid: a_h (semi-major axis), b_h (semi-minor axis), Sh_h (helix pitch), c_h (focal length of the ellipse), e_h (eccentricity of the ellipse), l_h (circumference of the ellipse), and S_h (area of the ellipse).

	$2a_h$ (Å)	a_h (Å)	$2b_h$ (Å)	b_h (Å)	Sh_h (Å)	c_h (Å)	e_h	S_h (Å ²)	l_h (Å)	
T (K)	300	6.73	3.37	3.09	1.55	11.07	2.99	0.89	16.36	15.96
	240	6.73	3.37	3.05	1.52	11.09	3.00	0.89	16.11	15.91
	180	6.74	3.37	3.02	1.51	11.12	3.01	0.89	15.99	15.89
	130	6.75	3.37	2.99	1.50	11.13	3.02	0.90	15.85	15.87
	100	6.76	3.38	2.98	1.49	11.06	3.03	0.90	15.85	15.88
p (GPa)	0.16	6.65	3.33	3.03	1.51	11.28	2.96	0.89	15.82	15.74
	0.95	6.57	3.28	2.88	1.44	11.53	2.95	0.90	14.85	15.40
	1.3	6.57	3.28	2.83	1.42	11.58	2.96	0.90	14.60	15.35
	1.67	6.57	3.29	2.77	1.39	11.65	2.98	0.91	14.29	15.28
	2.27	6.53	3.27	2.72	1.36	11.67	2.97	0.91	13.96	15.15

Table S11. The assignment of the selected vibrational bands observed in FT-IR and Raman spectra of **SalImi**.

v FT-IR (cm ⁻¹)	v Raman (cm ⁻¹)	Assignment	Literature	v calc.* (cm ⁻¹)
3159	3165	v(N–H)	[1]	3180
3151	3152	v(N–H)	[1]	3168
1626	1630	v(C=C)	[1]	1644
1572	1567	v _{asym} (COO)	[1, 6]	1601
	1524	v(C–N)	[1]	1509
1486	1480	v(C–COO)	[1, 6]	1559
1462	1454	ring mode + δ(CNH)	[1]	1460
1388		v _{sym} (COO)	[1]	1354
1346		v(C–OH)	[1]	1323
905	912	γ(CCH)	[1]	908
890	896	δ(NCN)	[1]	892
859	855	γ(CNH)	[1]	862
808	807	δ(CCN)	[1]	780
757	759	δ(CCH)	[1]	751

*calculated normal modes of imidazolium and acid ions using ωB97XD/6-311++G(d,p) method; scaling factor of 0.97 was used.

Table S12. The assignment of the selected bands observed in Raman spectra in the phonon spectral range of **SalImi**.

v Raman (cm ⁻¹)	Assignment	Literature
136	v(N ⁺ –H···O ⁻)	[2-5]
99	v(N ⁺ –H···O ⁻)	[2-5]
53	γ(N ⁺ –H···O ⁻)	[2-5]
40	γ(N ⁺ –H···O ⁻)	[2-5]

References

- (1) Zięba, S.; Dubis, A. T.; Gzella, A. K.; Ławniczak, P.; Pogorzelec-Glaser, K.; Łapiński, A. Toward a new type of proton conductor based on imidazole and aromatic acids. *Phys. Chem. Chem. Phys.* **2019**, *21*, 17152–17162.
- (2) Lippert, E. *Hydrogen Bond* (Eds.: M. D. Joesten, L. J. Schaad, M. Dekker) New York, **1974**.
- (3) Calderwood, J. H. The Hydrogen Bond. *Phys. Bull.* **1977**, *28*, 130.
- (4) D. Hadži, *Theoretical Treatment of Hydrogen Bonding*, Wiley, **1997**.
- (5) Widelicka, M.; Pogorzelec-Glaser, K.; Pankiewicz, R.; Łapiński, A. Spectroscopic investigations of the new anhydrous proton-conducting compound of pyrazole with oxalate acid. *J. Raman Spectrosc.* **2019**, *50*, 1914–1925.
- (6) Chinnakannu, E.; Sankar, M.; Chandran, S.; Thamotharan, K.; Manickam, S. Crystal growth, structural, optical, thermal, DFT and Z-scan analyses of Imidazolium 3,4-dinitrobenzoate crystal, *Journal of Molecular Structure*, **2023**, *1294*, 136419.

Table S13. Lengths and angles of the bonds in the imidazole ion as a function of the temperature. Note: The atomic labeling scheme is shown in Figure S2.

	100 K	130 K ^[1]	180 K	240 K	300 K
Bond Lengths (Å)					
N1a-C1a	1.324	1.323	1.316	1.311	1.306
N2a-C1a	1.329	1.327	1.324	1.319	1.319
N1a-C3a	1.371	1.366	1.358	1.349	1.342
N2a-C2a	1.367	1.361	1.353	1.344	1.342
C2a-C3a	1.347	1.340	1.329	1.317	1.308
Angles (°)					
N1a-C1a-N2a	108.5	108.4	108.3	108.3	108.2
C1a-N1a-C3a	108.6	108.6	108.6	108.5	108.5
C1a-N2a-C2a	108.6	108.5	108.3	108.0	107.8
N1a-C3a-C2a	107.0	107.1	107.1	107.1	107.4
N2a-C2a-C3a	107.2	107.4	107.6	108.0	108.1

Table S14. Lengths and angles of the bonds in the imidazole ion as a function of the pressure. Note: The atomic labeling scheme is shown in Figure S2.

	0.16 GPa	0.95 GPa	1.3 GPa	1.67 GPa	2.27 GPa
Bond Lengths (Å)					
N1a-C1a	1.392	1.327	1.296	1.299	1.299
N2a-C1a	1.341	1.289	1.297	1.287	1.299
N1a-C3a	1.398	1.361	1.383	1.416	1.298
N2aC2a	1.277	1.258	1.317	1.342	1.296
C2a-C3a	1.402	1.364	1.348	1.352	1.298
Angles (°)					
N1a-C1a-N2a	100.2	105.9	108.5	108.3	107.9
C1a-N1a-C3a	115.6	109.6	110.7	111.8	107.9
C1a-N2a-C2a	113.1	112.2	108.1	108.2	108.1
N1a-C3a-C2a	97.5	103.0	101.7	99.7	108.1
N2a-C2a-C3a	113.1	109.2	111.0	111.9	107.9